Online Journal of Space Communication

Volume 5
Issue 9 *Global Navigation Satellite System (Winter 2006)*

Article 13

Navigation Errors Introduced By Ground Vehicle Dynamics

William Travis

David M. Bevly

Navigation Errors Introduced By Ground Vehicle Dynamics

William Travis, *Auburn University*
David M. Bevly, *Auburn University*

BIOGRAPHY

William Travis is pursuing a M.S. in Mechanical Engineering from Auburn University. He graduated from Auburn with a B.S. in M.E. in 2004. He works in the GPS and Vehicle Dynamics Lab studying navigation of unmanned vehicles.

David M. Bevly is an assistant professor at Auburn University and head of the GPS and Vehicle Dynamics Lab. He received his PhD in Mechanical Engineering from Stanford University in 2001, his M.S. in M.E. from Massachusetts Institute of Technology in 1997, and his B.S. in M.E. from Texas A&M University in 1995.

ABSTRACT

An analysis of navigational accuracy when influenced by ground vehicle dynamics is presented. Tests beds outfitted with various sensor suites were used to collect data when normal and extreme driving maneuvers are executed. The data was run through an extended Kalman filter to produce a navigation solution. The Kalman filter inputs varied on each test bed, using both automotive and tactical grade Inertial Measurement Units (IMU). The position, velocity, and course measurements were obtained from a DGPS unit mounted on the vehicles and used as a truth measurement when exploring dead reckoning error. Additional measurements, such as wheel speed, radar speed, and magnetometer heading, were added to improve the robustness and reliability of the solution. The results of the work show the effect of both longitudinal and lateral vehicle slip on the navigation solution. In addition, the attempt of the various sensors to correct the errors is investigated.

INTRODUCTION

Accurate ground vehicle navigation is in an ever increasing demand as the market for autonomous capability continues to grow. Control of an autonomous ground vehicle (AGV) requires precise navigation information. An increase in the precision of the navigation solution can directly lead to a better and more robust vehicle controller.

Position information is important to both navigation experts and vehicle dynamicists. Sometimes, AGV navigation uses a vehicle model that neglects or constrains key states present in the actual dynamics of the ground vehicle at normal operating speeds [1], [2]. Vehicle dynamic models, however, can be excessively complicated for navigational use and can require parameters that are expensive or hard to measure. There exists a tradeoff in that some of these states need to be taken into account for accurate AGV navigation, vehicle platooning, and for the next generation of control systems in automobiles [3], [4], [5]. Active control systems that steer the vehicle away from an impending accident will generate large amounts of vehicle slip in order to maximize the force at the ground to quickly alter the vehicle's path and minimize the chance of a collision.

The focus of this work is to show how vehicle slip induces errors in the navigation solution both when GPS is available and when dead reckoning through a GPS outage. The drawbacks of typical navigation sensors when lateral or longitudinal slip occurs are detailed, showing that sensor errors can be a function of the environment and/or vehicle dynamics.

TEST BED

Two test beds were used for this research. The first was an Infiniti G35 sedan, donated by Nissan. It was outfitted with a Crossbow VG400 automotive grade inertial measurement unit (IMU), Navcom Starfire DGPS, and a Dickey John Doppler radar. Wheel speed from each wheel was taken from the vehicle's Control Area Network (CAN).

The second test bed for this research was an All-Terrain Vehicle (ATV) converted into an AGV used to participate in the DARPA Grand Challenge (DGC). It was outfitted with a Navcom Starfire DGPS unit, a Rockwell Collins GIC-100 tactical grade IMU, a Peiseler high resolution

wheel encoder, a Microstrain 3DM-GX1 IMU with magnetometer, and a second magnetometer.

NAVIGATION ALGORITHM

An extended Kalman filter (EKF) was used due to the nonlinearities in the system model. The filter used is a continuous-discrete hybrid filter formally known as an extended Kalman-Bucy filter. This is a widely used estimator when dealing with sampled data measurements of a continuous process. This method and the following equations are described in more detail in [6].

State Estimate Continuous Propagation

$$\hat{x}(t_k^-) = \hat{x}(t_{k-1}^+) + \int_{t_{k-1}}^{t_k} f\left[\hat{x}(\tau^-), u(\tau), \tau\right] d\tau \tag{1}$$

Covariance Estimate Continuous Propagation

$$P(t_k^-) = P(t_{k-1}^+) + \int_{t_{k-1}}^{t_k} \left[A(\tau)P(\tau) + P(\tau)A(\tau)^T + B_w(\tau)Q(\tau){B_w}^T\right] d\tau \tag{2}$$

Kalman Filter Gain Calculation

$$L(t_k) = P(t_k^-)C(t_k)^T\left[C(t_k)P(t_k^-)C(t_k)^T + R(t_k)\right]^{-1} \tag{3}$$

State Estimate Discrete Update

$$\hat{x}(t_k^+) = \hat{x}(t_k^-) + L(t_k)\left[y(t_k) - C(t_k)\hat{x}(t_k^-)\right] \tag{4}$$

Covariance Estimate Discrete Update

$$P(t_k^+) = \left[I - L(t_k)C(t_k)\right]P(t_k^-) \tag{5}$$

A specific kinematic system model was derived for each vehicle. The G35 model only estimates necessary to produce a navigation solution. The system model for the AGV is a prototype of the one being used in the actual DGC, and is more complex and contains more states. Both contain the following states required for navigation: position, velocity, and yaw. States specific to each test bed are listed in Equations (6) and (7) and are detailed in the appendix. Inputs for the G35 are the longitudinal acceleration and yaw rate, with scale factors removed. The AGV adds pitch rate and roll rate inputs.

$$x_{G35} = \begin{bmatrix} V & \psi & b_r & N & E & b_{ax} & b_{ws} & b_{dop} \end{bmatrix}^T \tag{6}$$

$$x_{AGV} = \begin{bmatrix} V & \psi & b_r & N & E & \phi & b_\phi & \ldots \\ & \theta_p & b_\theta & \theta_{rg} & b_{M\psi} & b_{M\phi} & b_{M\theta} & \ldots \\ & b_{M\psi 2} & b_{M\phi 2} & b_{M\theta 2} \end{bmatrix}^T \tag{7}$$

The Jacobian for each system used in the continuous propagation of the covariance estimate is listed in equations 8 and 9. The matrices are 8 x 8 for the G35 and 16 x 16 for the AGV, and are zero except where noted.

$$\begin{aligned} &A_{G35}(1,6) = -1 && A_{G35}(4,2) = -\hat{V}\sin(\hat{\psi}) \\ &A_{G35}(2,3) = -1 && A_{G35}(5,1) = \sin(\hat{\psi}) \\ &A_{G35}(4,1) = \cos(\hat{\psi}) && A_{G35}(5,2) = \hat{V}\cos(\hat{\psi}) \end{aligned} \tag{8}$$

$$\begin{aligned} &A_{AGV}(1,8) = -g && A_{AGV}(5,1) = \sin(\hat{\psi}) \\ &A_{AGV}(1,10) = -g && A_{AGV}(5,2) = V\cos(\hat{\psi}) \\ &A_{AGV}(2,3) = -1 && A_{AGV}(6,7) = -1; \\ &A_{AGV}(4,1) = \cos(\hat{\psi}) && A_{AGV}(8,9) = -1; \\ &A_{AGV}(4,2) = -\hat{V}\sin(\hat{\psi}) \end{aligned} \tag{9}$$

Measurements on the G35 include velocity, course, north, and east from GPS, and a wheel speed velocity from the CAN. The wheel speed velocity was translated to the CG. The measurement matrix is a 6 x 8 zero matrix except as noted below:

$$\begin{aligned} &C_{G35}(1,1) = 1 && C_{G35}(5,5) = 1 \\ &C_{G35}(2,1) = 1 && C_{G35}(6,1) = 1 \\ &C_{G35}(3,2) = 1 && C_{G35}(2,7) = 1 \\ &C_{G35}(4,4) = 1 && C_{G35}(6,8) = 1 \end{aligned} \tag{10}$$

The AGV used GPS measurements of velocity, course, north, east, and pitch plus road grade; magnetometer measurements of heading, roll, and pitch; a wheel speed velocity; and a roll "measurement" calculated using Equation (11). These measurements result in a measurement matrix for the AGV that is 13 x 16 and is zero except where noted.

$$\phi_k = \frac{1}{g}\left(a_{y(k)} - \hat{V}_k(r_k - b_{r(k)})\right) \tag{11}$$

$$\begin{aligned} &C_{AGV}(1,1) = 1 && C_{AGV}(6,12) = 1 \\ &C_{AGV}(2,1) = 1 && C_{AGV}(7,6) = 1 \\ &C_{AGV}(12,2) = 1 && C_{AGV}(7,15) = 1 \\ &C_{AGV}(12,11) = 1 && C_{AGV}(8,6) = 1 \\ &C_{AGV}(13,2) = 1 && C_{AGV}(9,8) = 1 \\ &C_{AGV}(13,14) = 1 && C_{AGV}(9,13) = 1 \\ &C_{AGV}(4,4) = 1 && C_{AGV}(10,8) = 1 \\ &C_{AGV}(5,5) = 1 && C_{AGV}(10,16) = 1 \\ &C_{AGV}(6,6) = 1 && C_{AGV}(11,10) = 1 \end{aligned} \tag{12}$$

The statistical properties of the noise were found by performing static tests and calculating the mean and variance of each sensor. The biases are modeled as slowly varying using the process noise matrix to dissuade the filter from "going to sleep."

VEHICLE SLIP

The tire is the vehicle's interface with the road. It is the component responsible for transferring the drive force to the ground and for generating the necessary lateral forces to turn the vehicle. Using a similar explanation as [7], parts of the tire tread are either adhered to the road or they are sliding. When a force from the vehicle is applied to the tire/road interface, the coefficients of friction are exceeded in local areas on the tread. Those areas begin to slide which generates a force to propel the vehicle. The force generated increases fairly linearly with slip until the tire becomes saturated, after which the force stays constant. The saturation limit of the tire is often defined by its effective stiffness. The cornering stiffness (C_α) and tractive stiffness (C_x) are functions of numerous parameters such as normal force, camber, toe, road conditions, materials, and so forth, but are not exactly known due to the high nonlinearities in tire behavior. Often empirical lookup tables or empirical models such as Pacejka's Magic Model are used to model the tire. Ultimately, vehicle drive forces are a function of the tire stiffness and lateral and longitudinal slip (α and s, respectively) at the tire in the linear region. In Equations (13) and (14), s is the slip due to the difference in wheel speed and vehicle speed, and α is the slip due to the difference in the tire pointing direction and the direction of travel.

$$F_x = C_x s \tag{13}$$

$$F_y = C_\alpha \alpha \tag{14}$$

These slip angles, in reality, are translated to the center of gravity of the vehicle to produce an overall vehicle slip angle. In practice, it is easier to measure or estimate this slip angle and translate it back to the individual tires for analysis or to gather other information [7], [8], [9], [10].

Vehicles are sometimes modeled kinematically with assumptions of zero lateral velocity, no wheel slip, and the existence of a direct relationship between steer angle and yaw rate. At low speeds, these assumptions may be valid. At higher speeds or on varying terrains, these assumptions quickly break down resulting in undesired performance from navigation and/or control algorithms. Lateral velocities are generated and the vehicle sideslip becomes large enough to impact the system. Vehicle sideslip is formally defined as the angle between the vehicle's heading vector and the vector that denotes the vehicle's actual path of travel. (the angle β in Figure 1). High speed is also a term that is particular to each vehicle and the ground it is traversing. For example, 10 mph is fairly low speed in the sedan but fast enough to create sizeable slip angles in the AGV. Terrain is a critical factor that drastically changes the available peak forces of the tire, which are located in the nonlinear region of the tire curve. This too, can change the relative meaning of the term high speed. While 10 mph is certainly low speed on level pavement, it would not be under certain icy conditions and the vehicle would generate much larger slip angles and saturate the tires faster. Figure 1 is a simple four wheel vehicle model that depicts the noted parameters that induce errors in control and navigation systems. The variable descriptions are offered in the appendix.

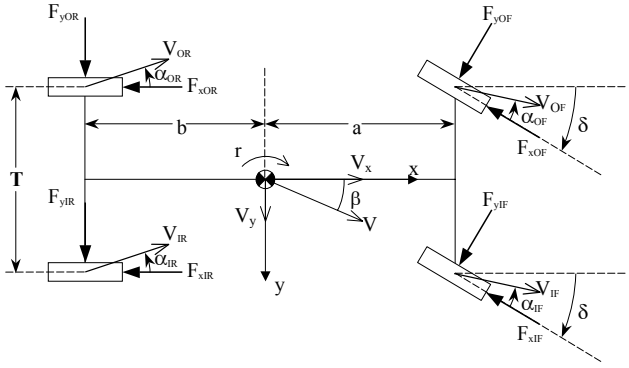

Figure 1: A simple four wheel vehicle model.

A broad range of sensors are available to measure most, if not all, of the parameters shown. Encoders and potentiometers are effective when measuring steer angle, an IMU will provide yaw rate, strain gauges will measure the forces generated, and magnetometers provide heading. GPS has proven to be an effective, economical tool to directly measure or to aid in estimating many vehicle parameters. A single antenna unit can give information such as precise velocity, position, and course measurements, while a multiple antenna unit provides more attitude information such as heading, roll, and pitch. Course is the angle between north and the direction of travel of the vehicle, and heading is the angle between north and the direction the vehicle is pointing. With a combination of a single and multi-antenna unit, sideslip can be directly measured. Wheel slip can also be measured by comparing GPS velocity to a wheel speed sensor.

Problems arise in the absence of GPS. The navigation system loses its "truth" measurement creating states that are undetectable and unobservable in some situations. Additionally, the estimator loses the ability to estimate states such as wheel slip. Biases inherent to most sensors are often unobservable during an outage, which increases dead reckoning error. These sensor errors can also be a function of the environment and/or vehicle dynamics. Terrain can cause significant changes in biases as well. A changing road grade will alter the accelerometer readings and appear as a large bias. The Doppler radar is affected when the vehicle rolls or pitches due to acceleration or

road grade because the distance and angle of the unit relative to the ground changes (the radar provides a speed measurement that is a function of the sensor's distance and angle relative to the ground). Changing from a loose surface to a hard surface affects the amount of wheel slip, which can be modeled as a bias in the longitudinal direction. Surface conditions also impact the Doppler radar output because the height and texture of different terrains alter the reflectivity of the microwave signal. Hard accelerations, braking, or cornering also inject errors because slip is generated longitudinally or laterally. A wheel speed sensor obviously has shortcomings in this scenario. Yaw errors are also present without a course measurement because integration of a yaw rate gyro is used to produce the heading state. Additionally, the navigation algorithm is incorrect in its estimation of the vehicle's direction of travel if sideslip is present because the yaw gyro integration yields heading, not course. If these biases or conditions perceived as sensor bias remain constant during an outage, the states they are linked to generally provide adequate solutions. A changing bias or terrain, however, will induce large errors that quickly increase the position errors.

EFFECTS OF LATERAL SLIP

A series of maneuvers were executed on Auburn University's 1.7 mile oval test track using the Infiniti G35 to generate varying amounts of sideslip. Small slip angles were generated going around the eight degree banked turn, while large amounts were generated in a slalom maneuver on the straight section as shown in Figure 2. The 180 degree turns are clearly visible on the east and west ends of the track. The vehicle's speed was approximately 15.6 meters per second (35 mph) in the corners and 20.1 m/s (45 mph) on the straight sections.

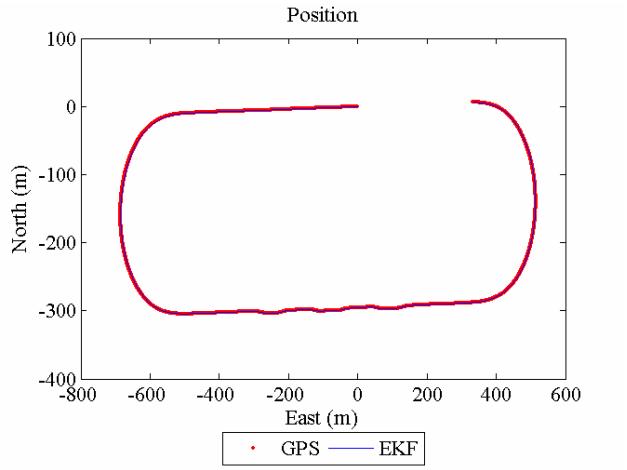

Figure 2: Overview of driving maneuvers on test track.

Figure 3 shows a zoomed in view of the southern straight away where the aggressive slalom maneuver was performed. The EKF navigation solution is denoted by the blue line, while the GPS waypoints are shown as red dots.

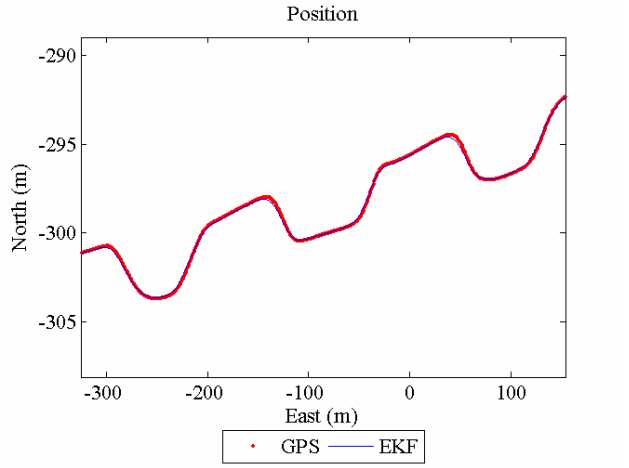

Figure 3: Close up of hard slalom maneuver on south straight section.

First, the EKF output when GPS was available was studied. Figure 4 displays the vehicle's course and the EKF output during the slalom. The vehicle's direction of travel is correctly estimated during the straight driving, but discrepancies exist during the slalom maneuver.

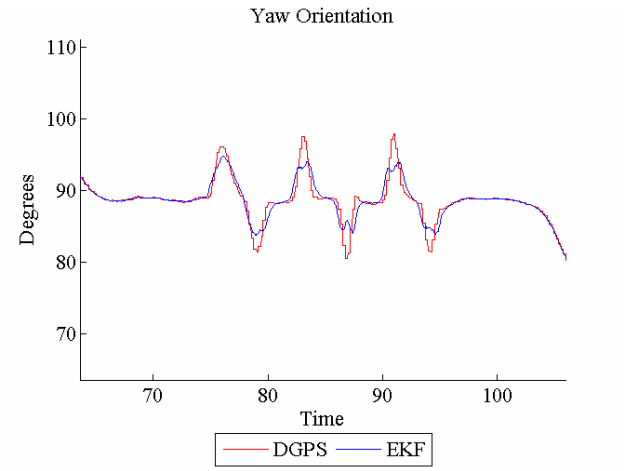

Figure 4: Vehicle yaw.

In order to understand the disagreement between the measurement and the estimate, the yaw rate gyro bias was examined. As seen in Figure 5, the bias estimate absorbed some of the generated sideslip. However, this phenomenon did not correct the error in the estimate. The level of filtering can be adjusted in the Kalman filter to let the estimate converge to the course measurement, but the bias estimate becomes increasingly incorrect. In other words, there exists a tradeoff between the performance of the EKF yaw state and yaw gyro bias state, which directly influences the dead reckoning estimation during a GPS outage.

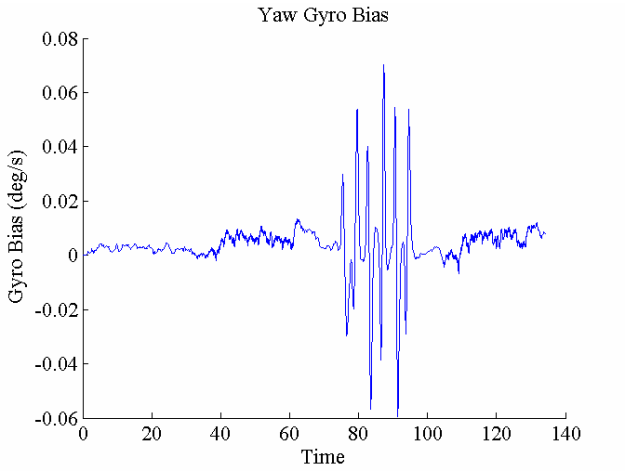

Figure 5: Estimate of the yaw gyro bias.

Position errors were larger than expected, especially on the 180 degree turns. This is due to the sideslip generated during each maneuver. Some systems will accept the level of error shown in Figure 6 (~40cm), but this is enough to exceed the tolerance of other systems. The small sideslip observed going around the 180 degree turn leads to a 40cm position error over 30 seconds. The sharp cornering leads to 30cm in less than a second. If this level of sideslip (~4 degrees) continued for an extended period of time or was larger, the position error would quickly exceed the tolerance of nearly any system.

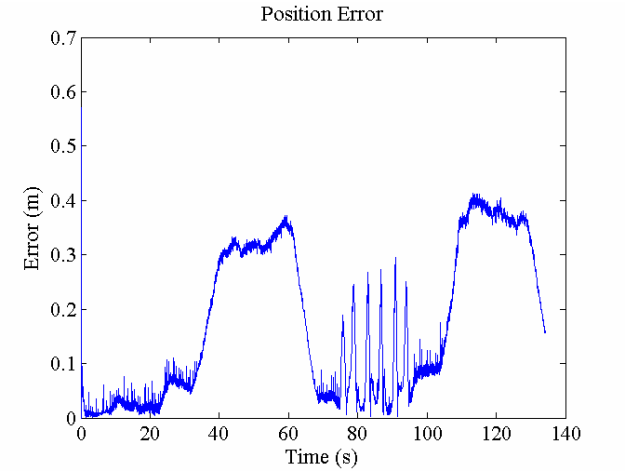

Figure 6: Position error due to lateral slip.

The next step in the investigation artificially removed GPS at two points in the run to demonstrate the influence of sideslip during an outage. GPS was removed just before entering turn one but after the EKF had settled. The yaw bias freezes (Figure 7) because it becomes unobservable when GPS is lost.

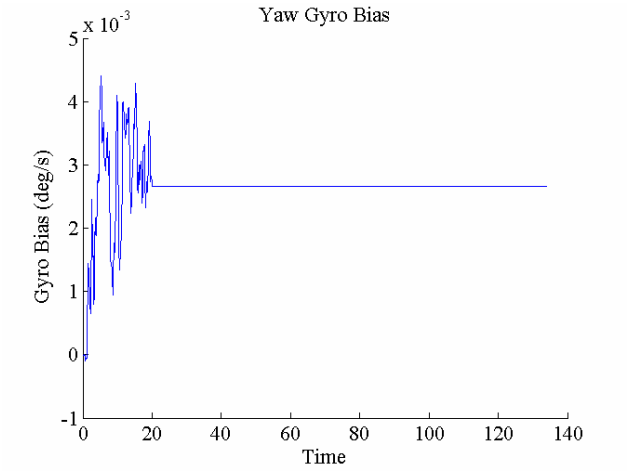

Figure 7: Yaw gyro bias during a GPS outage.

The navigation solution now contains two sources of error due to the inability to estimate the yaw gyro bias: random bias walk and vehicle sideslip. The effects of the error seem low when looking at the vehicle yaw estimate (Figure 8) but lead to unacceptable levels of position error (Figure 9).

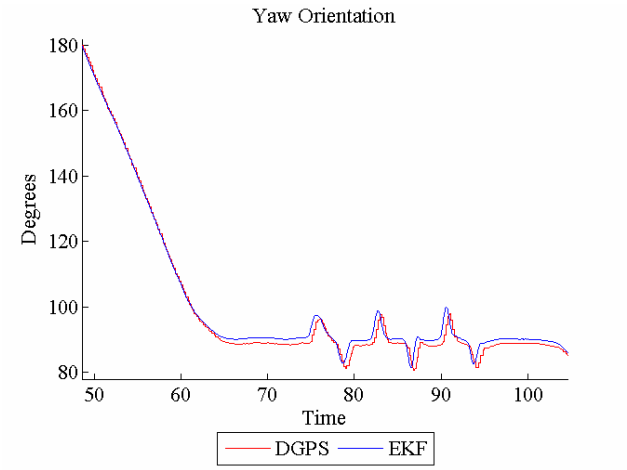

Figure 8: Yaw error due to sideslip and random bias walk during a GPS outage.

The green lines in Figure 9 outline the GPS outage. Error is approximately 5 meters after 20 seconds and 10 meters after 40 seconds. The DGC defines a 10 meter corridor the vehicle must travel through. A 20 second outage is all a vehicle with this sensor suite traveling at this speed could handle and still stay in contention. A highway vehicle has much more strict limitations because the corridor defined by the lane width is narrower. A 5 second outage is the maximum in a highway vehicle. Both scenarios assume the vehicle is traveling in the center of the corridor before the outage.

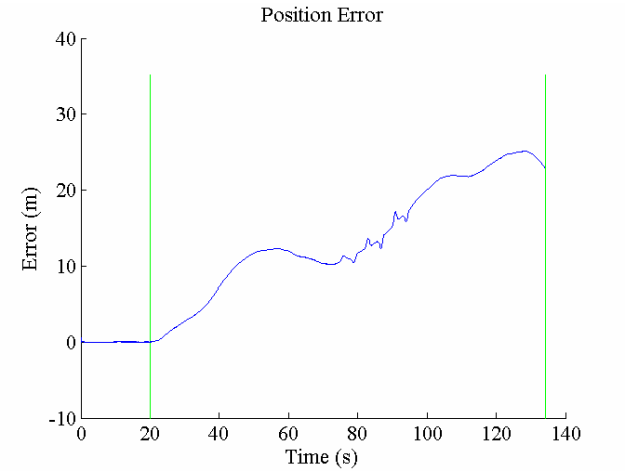

Figure 9: Position error due to random bias walk and sideslip.

Next, GPS was removed during times when the vehicle is producing large amounts of sideslip. This is the worst case scenario test but unfortunately is very plausible. Again, the yaw bias estimate freezes when GPS is lost (Figure 10). As shown previously when GPS was available, the yaw gyro bias estimate absorbs some vehicle sideslip. This causes the yaw gyro estimate to be incorrect when a GPS outage occurs during periods where vehicle sideslip is present.

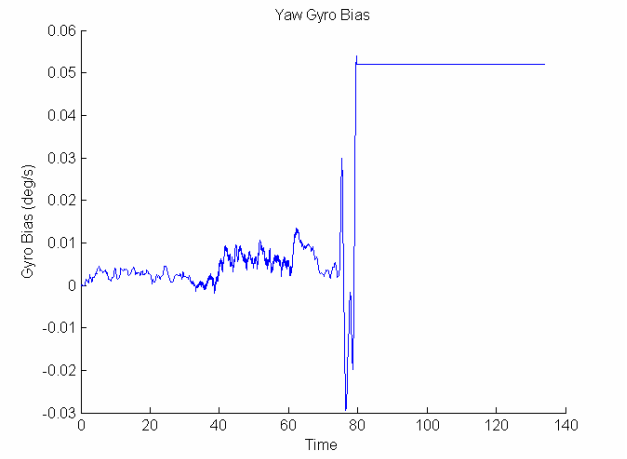

Figure 10: Yaw gyro bias estimate during a GPS outage.

The incorrect bias estimate turns into a linear error in the yaw estimate as seen in Figure 11, which is much larger than the previous scenario shown in Figure 8. The error sources of yaw now include sideslip, the inability to estimate a bias walk, and a bias offset due to slip.

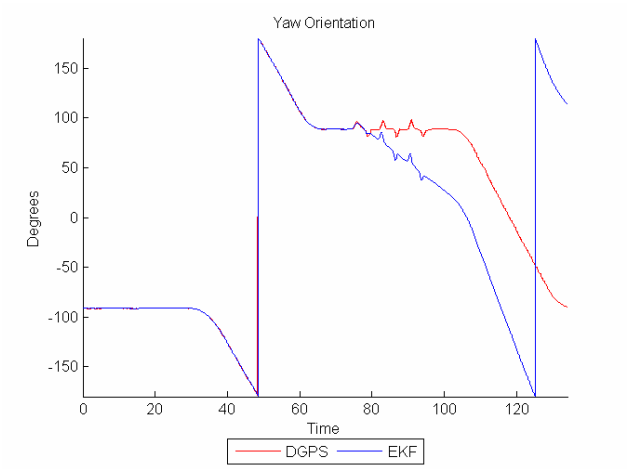

Figure 11: Yaw estimate during a GPS outage when sideslip is present.

Figure 12 shows the positional error during the simulated outage. The culmination of errors in the yaw gyro estimate propagates through the Kalman filter to almost instantly produce an unacceptable position estimate.

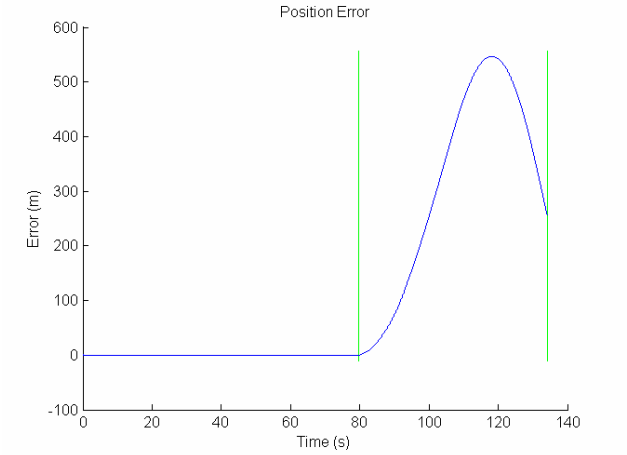

Figure 12: Large position error due to incorrect yaw gyro estimate during a GPS outage.

The AGV's sensor suite contained two magnetometers and a tactical grade IMU. The magnetometers were used as additional measurements in the Kalman filter, and the tactical IMU replaced the Crossbow's inputs. Figure 13 shows the output of all yaw sensors with the 16 state Kalman filter estimate of yaw during a 70 degree cornering maneuver that generated sideslip. The Microstrain magnetometer (denoted by Mag2) is very clean, but is heavily biased. The second magnetometer is noisy, but has a lower bias and substantially lower bias walk.

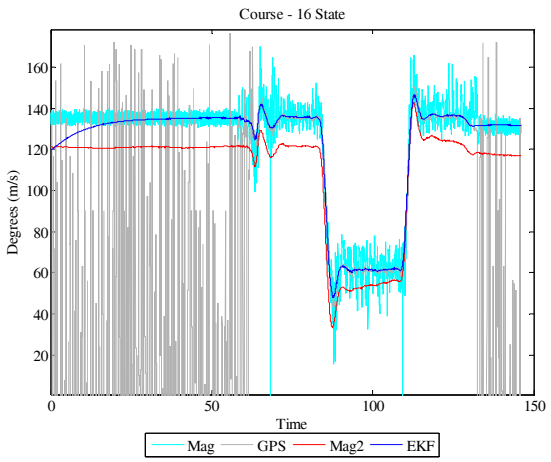

Figure 13: Outputs from GPS, magnetometers, and the 16 state KF.

Magnetometers are useful when initializing a vehicle's yaw orientation. However, they provide a measurement of heading, not course, and therefore the difference is absorbed in their bias estimates when GPS velocity measurements are used to calibrate the magnetometer. The effects seen in the Kalman filter during a GPS outage are similar to the integration of a yaw rate gyro during an outage. Figure 14 shows the GPS course, the output of the 16 state KF, and the output of the 16 state KF with the magnetometers turned off. A GPS outage was simulated starting at 75 seconds. The two Kalman filter outputs virtually lie on top of one another, but there is still a discrepancy between the estimated course and GPS course due to sideslip. Since the change in position depends on the direction of travel of the vehicle (course), this leads to a positional error. Additionally, this demonstrates the potential for large errors when more sideslip is generated or when slip occurs more frequently.

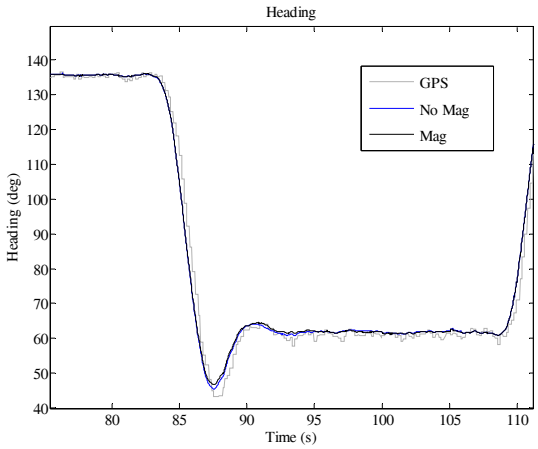

Figure 14: Estimator outputs with and without magnetometer measurements during an outage.

EFFECTS OF LONGITUDINAL SLIP AND TERRAIN

Wheel slip in the longitudinal direction can also be devastating to the accuracy of the navigation solution when using a wheel speed sensor as a redundant measurement of velocity. Figure 15 displays the corrupted navigation solution when wheel slip is not accounted for in the estimator while GPS is available.

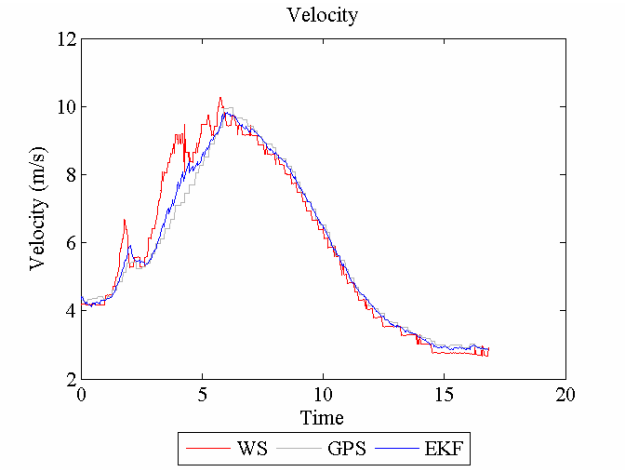

Figure 15: Corrupted velocity estimate due to wheel slip.

The slip can be modeled as a bias to remove its undesired effects when GPS is available, but during a GPS outage the velocity estimate can degrade to unacceptable performance levels if the amount of slip changes. Figure 16 shows the velocity when wheel slip is modeled as a bias. A GPS outage was simulated starting at 4 seconds. Until the outage, the estimator performs well and lines up with GPS velocity. After the outage, the amount of slip varies and the bias estimate shown in Figure 17 is incorrect. This leads to an incorrect velocity estimate. The EKF still attempts to estimate the wheel speed bias using the longitudinal accelerometer for a few iterations after the outage but eventually settles out and goes to sleep. This area requires further investigation to see why the bias is still detectable during the initial part of the outage.

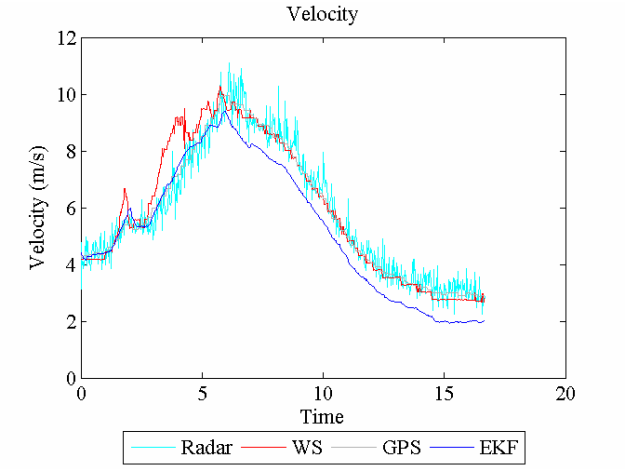

Figure 16: Velocity taking wheel slip into account and simulating an outage.

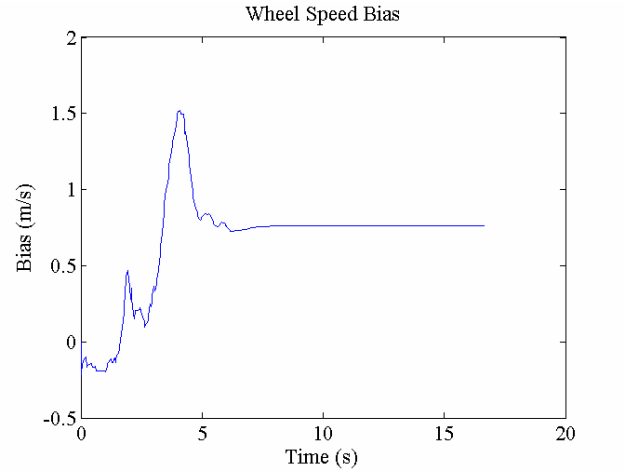

Figure 17: Wheel speed bias showing slip and during an outage.

A Doppler radar is a common speed sensor and can be helpful on some terrains because it is insensitive to slip. A drawback to using radar is the bias is terrain dependent. The effect is similar to what happens when using a wheel speed sensor during moments of tire spin, except it can be more predictable and perhaps even given to the estimator as a priori knowledge. The G35 was driven on the paved track and on gravel to measure speed on two different terrains. The estimator was used to calculate the bias of the radar and is shown in Figure 18. In the constant speed section of the graph (25 to 60 seconds) the average bias difference from gravel to pavement is approximately 30 cm/s. This would induce a 3 meter error after 10 seconds of a GPS outage if a transition from one type of terrain to another type occurs. This plot also shows the radar's susceptibility to vehicle pitch. The test run on the pavement started with a period of hard acceleration. The vehicle pitch changes the height and angle of the sensor and induced a bias into the measurement. This quickly changing bias would produce large position errors in the event of a GPS outage. Uneven terrain would mimic this scenario by stimulating the cars suspension or providing an inconsistent height and angle of the radar relative to the ground.

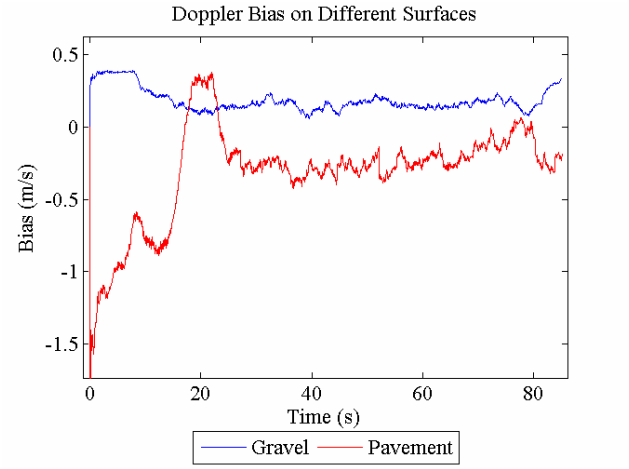

Figure 18: Radar bias when pitching and on different terrain.

After studying the major limitations of both the wheel speed sensor and the radar, a redundant Kalman filter was used to compare the error during an outage using each sensor alone and a combination of the sensors. The navigation algorithm estimated wheel speed bias and radar bias, and used the same run shown in Figure 16 which had moderate amounts of wheel slip. As expected, the EKF using only wheel speed generated the largest position error because of the large bias inaccuracy. The EKF using only the radar was more accurate than the previous scenario because the terrain remained fairly constant and the vehicle experienced minimal pitch. The last EFK utilizing both measurements provided the most accurate solution for the duration of the outage. The redundancy averages some of the errors to provide a better solution.

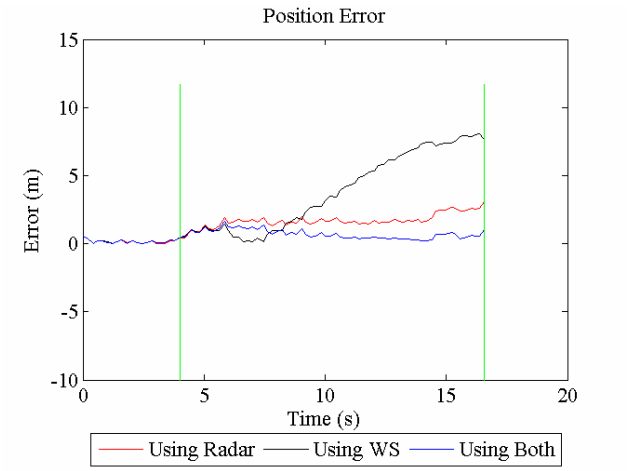

Figure 19: Position error using one additional measurement and using both measurements.

CONCLUSIONS

Several scenarios were presented where lateral vehicle slip produced position errors in the navigation solution with and without GPS. When GPS was available, the introduced errors were small and manageable by most systems. However, the errors were significant when an outage occurred, especially when the outage occurred while slip was generated. A magnetometer was used as a supplemental measurement, but was found to be ineffective when trying to reduce the error due to slip because it provides a measurement of heading, not course.

Additional sensors can be used to obtain the course measurement during an outage, but can become quite costly. Optical sensors will provide velocities in the x and y direction (in the vehicle frame), and some radar speed sensors are sensitive enough to measure lateral velocity. Previous work has shown a Lidar can be used to measure lateral error and slip [11]. Another possible solution is to use a model based estimator to estimate the sideslip as shown in [12], but this method requires accurate knowledge of some vehicle parameters which are often difficult to obtain. When GPS is available, a multi-antenna receiver can measure sideslip to further increase the accuracy of the estimate.

In the longitudinal direction, scenarios were presented that expose the shortcomings of typical dead reckoning sensors. A wheel speed sensor can aid in estimating velocity when the wheel slip is taken into account, and can handle GPS outages well if slip remains constant. When slip varies, the bias estimate becomes corrupted and increases the position error. Similarly, a Doppler radar can provide adequate ground speed measurements during a GPS outage unless the terrain on which the vehicle is traveling changes. The radar speed bias is a function of terrain, and is not observable during an outage.

ACKNOWLEDGMENTS

Special thanks to Nissan for the Infiniti G35 and to SciAutonics for the partnership in the Grand Challenge effort.

REFERENCES

[1] G. Dissanayake, S. Sukkarieh, "The Aiding of Low-Cost Strapdown Inertial Measurement Unit Using Vehicle Model Constraints for Land Vehicle Applications," IEEE Transactions on Robotics and Automation, vol. 17, no. 5, pp. 731-747, Oct. 2001.

[2] S. Godha, M. Cannon, "Integration of DGPS with a Low Cost MEMS – Based IMU for Land Vehicle Navigation Application," Proceedings of the ION GNSS 2005, Sept. 2005.

[3] B. He, D. Wang, M. Pham, T. Yu, "GPS/Encoder Based Precise Navigation for a 4WS Mobile Robot," Seventh International Conference on Control, Automation, Robotics, and Vision (ICARCV), Dec. 2002.

[4] J. Zuurbier, P. Bremmer, "State Estimation for Integrated Vehicle Dynamics Control," TNO Automotive.

[5] R. Daily, D. Bevly, "The Use of GPS for Vehicle Stability Control Systems," IEEE Transactions on Industrial Electronics, vol. 51, no. 2, April 2004.

[6] R. Stengal, *Optimal Control and Estimation,* Dover Publications, Mineola, NY, 1994, ISBN: 0-486-68200-5.

[7] D. Milliken, W. Milliken, *Race Car Vehicle Dynamics,* Society of Automotive Engineers, Warrendale, PA, 1995, ISBN: 1-56091-526-9.

[8] T. Gillespie, *Fundamentals of Vehicle Dynamics,* Society of Automotive Engineers, Warrendale, PA, 1992, ISBN: 1-56091-199-9.

[9] J. Dixon, *Tires, Suspension, and Handling,* Society of Automotive Engineers, Warrendale, PA, 1996, ISBN: 1-56091-831-4.

[10] B. Olson, S. Shaw, G. Stépán, "Nonlinear Dynamics of Vehicle Traction," Vehicle System Dynamics, vol. 40, no. 6, pp. 377-399, 2003.

[11] W. Travis, A. Simmons, D. Bevly, "Corridor Navigation with a Lidar/INS Kalman Filter Solution," IEEE Intelligent Vehicle Conference 2005, June 2005.

[12] R. Anderson, "Using GPS for Model Based Estimation of Critical Vehicle States and Parameters," MS Thesis, Auburn University, Department of Mechanical Engineering, Dec. 2004.

APPENDIX

F_x - Longitudinal force
F_y - Lateral force
IF/R – Inner front/rear
OF/R – Outer front/rear
T – Track width
a/b – Distance from the front/rear axle to CG
r – Yaw rate
δ – Steer angle
A – Tire slip angle
B – Sideslip
V – Velocity

b_{ax} – Longitudinal accelerometer bias
b_{dop} – Doppler radar bias
2 – Microstrain magnetometer
Ψ – Vehicle yaw
θ_p – Vehicle pitch + longitudinal accelerometer bias
$b_{M\psi/\varphi/\theta}$ – Magnetometer yaw/roll/pitch bias
b_{ws} – Wheel speed bias
φ – Vehicle roll + lateral accelerometer bias
θ_{rg} – Road grade
b_r – Yaw gyro bias

b_φ – Roll gyro bias
N – North position
b_θ – Pitch gyro bias
E – East position